Detection of trends in magnitude and frequency of flood peaks across Europe

Detection of trends in magnitude and frequency of flood peaks across Europe

Walter Mangini [a], Alberto Viglione [a], Julia Hall [a],

Yeshewatesfa Hundecha [b], Serena Ceola [c], Alberto Montanari [c],

Magdalena Rogger [a], Jose Luis Salinas [a], Iolanda Borzì [d], Juraj Parajka [a*]

[a] *Institute of Hydraulic Engineering and Water Resources Management, Vienna University of Technology, Karlsplatz 13 E222/2, 1040, Vienna, Austria.*

[b] *Swedish Meteorological and Hydrological Institute, Folkborgsvägen 17, 601 76, Norrköping, Sweden.*

[c] *Department of Civil, Chemical, Environmental and Material Engineering, University of Bologna, Viale Risorgimento 2, 40136, Bologna, Italy.*

[d] *Department of Engineering, University of Messina, Piazza Salvatore Pugliatti 1, 98122, Messina, Italy.*

*Corresponding author: Juraj Parajka,

Tel: +43-1-58801-22311, e-mail address: parajka@hydro.tuwien.ac.at,

Postal address: J. Parajka at TU Wien E222/2, Karlsplatz 13, 1040, Vienna, Austria

Detection of trends in magnitude and frequency of flood peaks across Europe

This study analyses the differences in significant trends in magnitude and frequency of floods obtained from Annual Maximum Flood (AMF) and Peak Over Threshold (POT) flood peak series. Flood peaks are identified from European daily discharge data for the period 1965-2005, using a baseflow-based algorithm and significant trends in AMF series are compared with POT series, derived for six different exceedance thresholds. Results show that more trends in flood magnitude are detected in the AMF than the POT series and for the POT series more significant trends are detected in flood frequency than in flood magnitude. Spatial coherent patterns of significant trends are detected, which is further investigated by stratifying the results into five regions based of catchment and hydro-climatic characteristics. All data and tools used in this study are open-access and results are fully reproducible.

Keywords: Annual Maximum Flood, Europe, flood frequency, flood magnitude, Peak Over Threshold, trend.

Highlights: Consistent regional patterns of significant trends in flood magnitude and flood frequency are detected across Europe using freely available daily discharge time series. Flood trends are sensitive to the method used to define the flood peak series. The paper supports the value of open data and tools for the advance of hydrological science, ensuring the full reproducibility of the analyses.

41 ## 1. Introduction

42 Recently, numerous extreme flood events have been recorded across the European
43 continent, such as the central European floods in summer 2002 and 2013 (Ulbrich et al.
44 2003, Blöschl et al. 2013, Schröter et al., 2015), floods in England in summer 2007 and
45 winter 2013 (Marsh 2008, Muchan et al. 2015) and flash flooding in western Italy in
46 autumn 2011 (Marchi et al., 2013). As many of these and other recent flood events are
47 perceived unprecedented, there is a growing concern that flooding in Europe has
48 become more frequent and severe.

49 Accounting for possible changes in floods is important for hydrological
50 applications, such as design of flood protection facilities, risk assessment and risk
51 management (Parry et al. 2007, Kundzewicz 2012, Rosner et al. 2014). Additionally,
52 accounting for temporal trends in flood peak series may lead to better flood frequency
53 estimates (Khaliq et al. 2006, Renard et al. 2006, Vogel et al. 2011, Šraj et al. 2016).

54 To detect changes in floods, several analyses have been performed for different
55 regions in Europe. Examples of recent studies include but are not limited to: Hannaford
56 and Buys (2012) for Great Britain, Murphy et al. (2013) for Ireland, Giuntoli et al.
57 (2012) in France, Arheimer and Lindström (2015) in Sweden, Blöschl et al. (2011) and
58 Jeneiova et al. (2016) in Austria, Brázdil et al. (2006, 2012), Kundzewicz et al. (2013)
59 and Pekárová et al. (2016) in the Central Europe, and Bard et al. (2012) for the Alpine
60 mountain range region. Such analyses provided insight into regional patterns of flood
61 changes within selected catchment, national or regional boundaries. Hall et al. (2014)
62 performed a meta-analysis of published literature on flood change across Europe. They
63 found large-scale patterns of flood changes with similar sign of change but also
64 concluded that the studies are not fully comparable, due to different time periods

65 analysed and differences in the methodology applied to derive flood series and to detect
66 flood changes.

67 When performing trend tests on flood series, the main methodological concerns
68 include the definition of the variable "flood". Commonly two different methods are
69 used to derive times series of flood peaks, the Annual Maximum Flood (AMF) series
70 and the Peak Over Threshold Flood (POT) series. The AMF series consists of the
71 largest discharge values per each year, with the main advantage that the events selected
72 in two successive years are generally considered independent. However, the AMF
73 approach does only consider a small number of flood peaks and does not take into
74 account the flood events that are lower than the annual maximum, but may be relevant
75 to society, particularly in terms of damages.

76 The POT series (also denoted as Partial Duration Series), consists of flood peaks
77 exceeding a predefined threshold (Cunnane 1973, Madsen et al. 1997). If the POT series
78 is used, it is important to ensure that the peaks are independent (e.g. do not occur on the
79 recession curves of the preceding flood peak). The advantage of the POT compared to
80 the AMF series is that it allows not only the detection of trends in the mean magnitude
81 of flood peaks exceeding a threshold (trends in magnitude) but also trends in the mean
82 number of flood events per year (trends in frequency).

83 Large-scale studies using the POT flood series with high spatial resolution do
84 not exist in Europe so far. An example of a continental scale study can be found in
85 Hirsch and Archfield (2015) and Archfield et al. (2016) for the US. The authors found
86 no consistent national wide trend in the flood series signal but some regional trend
87 pattern. In Europe, there are examples of studies aiming to characterise changes in
88 floods adopting the POT approach, but those analyses use either high spatial resolution
89 databases at a regional scale (Petrow and Merz 2009, Vormoor et al. 2016) or

90 continental database with only a small number of stations (Mediero et al. 2015). In all
91 these studies, the threshold values for the selection of the POT series have been chosen
92 by fixing a mean number of events per year or per season (in general 1, 2 or 3 events)
93 but, to our knowledge, no systematic analysis to detect the effect of the threshold
94 selection on the trend detection results together with their spatial patterns was
95 performed so far. Méndez et al. (2006) underlines that: "The selection of the threshold
96 implies a balance between bias and variance. Too low a threshold will likely violate the
97 basis of the model, causing bias; too high a threshold will identify few extremes, leading
98 to high variance".

99 The main objective of this paper is therefore to detect trends across Europe,
100 derived from AMF and POT flood peaks series. The following research questions are
101 being addressed:

102 (1) What are the patterns of trends in both flood magnitude and frequency across
103 Europe for the period 1965-2005?
104 (2) What is the sensitivity of the detected trends to the selection criterion used to
105 define different flood peak series?
106 (3) What are the larger scale morpho-climatological characteristics of the
107 catchments with significant trends?

108 The analysis is performed on a large open-source dataset comprising 629 gauging
109 stations with daily mean discharges. All data and tools used here are open-access and
110 available at the SWITCH-ON portal (http://www.water-switch-on.eu).

111

112

2. Methodology

Changes in flood magnitude and frequency are detected by performing trend analysis on flood peak series. The flood peak series are compiled using a procedure based on (i) separating independent discharge events employing a baseflow separation algorithm, (ii) selecting the maximum daily discharge within each individual event as the peak event and (iii) sampling those events to be considered flood peaks, according to the different AMF or POT approaches. The first two parts of the methodology are described in section 2.1, the selection of flood peaks is elaborated in section 2.2 and the methodologies used for trend detection are presented in section 2.3.

2.1 Identification of independent peak events

Trend tests are based on the assumption that data are identically distributed and independent (WMO 2009). Two consecutive extreme events can be assumed physically independent when they are caused by different forces, so that the previous event does not condition the occurrence of the second event.

While the AMF approach leads to flood events that are generally considered independent, an objective selection criterion is needed within the POT approach for obtaining independent flood peaks. Generally, the independence criteria are related to the concept of streamflow recession, which states that the independence of two flood events increases over time if the discharge between them is decreasing.

Therefore, one possible criterion for defining temporal independence of the peaks within the POT series is to define a minimum number of days between two successive events, either by using a predefined value, e.g. 15 days (Mallakpour and Villarini 2015) or by determining a time lag as direct function of the catchment size

137 (Svensson et al. 2005). Another possible independence criterion that has been suggested
138 by the USWRC (1982), is the introduction of an additional condition concerning the
139 intermediate discharge magnitude between two successive peaks, as for example
140 applied in Mediero et al. 2015.

141 In the present work, the criterion of independence is fulfilled using a baseflow-
142 based algorithm. The algorithm allows the separation of independent discharge peak
143 events by comparing the recorded total flow and the estimated baseflow. The maximum
144 daily mean discharge within each separated event can then be considered an
145 independent discharge peak event.

146 The traditional procedure for the baseflow estimation starts with identification of
147 the points at which the direct runoff component of a hydrograph (i.e. surface runoff)
148 starts and, successively, ends. The start and end points are normally identified as the
149 point in time when the flow starts to increase, or a plot of logarithmic transformed
150 discharge values against time becomes a straight line, respectively.

151 In this study, the Chapman digital filter (Chapman 1999) was applied. The
152 digital filter estimates the baseflow as a simple weighted average of the direct runoff
153 and the baseflow at the previous time interval:

154 $$Qb(i) = k \cdot Q_b(i-1) + (1-k) \cdot Q_d(i) \quad (1)$$

155 where $Q_b(i-1)$ and $Q_d(i)$ are the baseflow at time interval i-1 and the direct runoff at time
156 interval i, respectively, and the parameter k is the recession constant during periods of
157 no direct runoff. Assuming that the recorded total flow Q(i) is the sum of baseflow $Q_b(i)$
158 and direct runoff $Q_d(i)$, then the $Q_b(i)$ can be estimated as:

159 $$Q_{b(i)} = \cdot Q_{b(i-1)} + \cdot Q_{(i)} \quad (2)$$

160 The estimation of the recession constant k for each catchment follows the
161 approach suggested in Vogel and Kroll (1996) and successive applications (Thomas et
162 al. 2013). The approach consists of the following steps:

163 (1) Identification of the start/end of the discharge recession, defined as the point in
164 time when a 3-day centred moving average begins to decrease/increase;
165 (2) Rejection of the recessions shorter than 10 days;
166 (3) Removal of the first three points of the recession to eliminate the effect of the
167 moving average;
168 (4) For each recession identified, a regression $\ln(Q) = \ln(Q_0) + \ln(k_i) \cdot t$ + residual is
169 fitted, applying the ordinary-least-squares method;
170 (5) Computing the average of the estimated regression slope k_i, for individual
171 events, to approximate the recession constant k.

172 Once the recession constant k is estimated, the baseflow Q_b is calculated using the
173 Chapman filter. The direct runoff Q_d is obtained as the difference between the recorded
174 total flow and the estimated baseflow. Discharge events are defined here as independent
175 if they are separated by intervals within which the direct runoff is lower than the
176 baseflow or lower than the mean annual direct runoff (to remove the instances when
177 discharge or baseflow equals zero). The maximum discharge value within each
178 discharge event is then selected as independent flood peak.

179 Fig. 1 shows a sample application of the baseflow-based algorithm for the peak
180 separation in the river Teme at Tembury, Western England (catchment area 1134 km^2)
181 for the year 1968. The figure shows the total discharge time series, the estimated
182 baseflow, the start and end points of the identified discharge event and the independent
183 flood peaks for each separated event.

184

185 ## 2.2 Selection of flood series

186 Flood series are compiled from the discharge peaks identified by the methodology in
187 Section 2.1 using two different approaches: the Annual Maximum Flood (AMF) and the
188 Peak Over Threshold (POT) selection approach.

189 AMF are commonly identified by a so-called "block maximum" approach
190 (Gumbel, 1958). This method requires the time series to be divided into blocks of equal
191 length and the largest value within each block to be selected. The main advantage of this
192 method is that the immediate correspondence with the "Return Period" concept can be
193 made, considering one year as time unit. One limitation of the method is that annual
194 peaks with very small values may be included (e.g. in drier years), whereas in years
195 with several larger floods only the largest value is considered.

196 The POT method identifies all flood events that exceed a given threshold. Unlike
197 the AMF approach, the POT methodology allows the analysis of both trends in
198 magnitude (POT-M) and trends in frequency (POT-F).

199 When performing trend analysis on flood series using the POT approach, the
200 number of floods to be included in the series is determined by selecting an appropriate
201 threshold. Many studies use a fixed mean number of exceedances per year (λ) to
202 identify the appropriate threshold value. In the specific case of this study, the length of
203 the time series analysed is 41 years: if λ is chosen to be one (POT1), the highest 41
204 discharge peaks are considered to form the flood series. By formulating the hypothesis
205 that flood events follow a Poisson process, λ represents the event rate (or frequency) per
206 unit time of the distribution.

207 In this paper, the sensitivity of the trend results to the selection of the threshold
208 is assessed for a mean number of exceedances per year λ ranging from one to six (POT1
209 to POT6). Additionally, trends in the flood magnitude series of POT1 are compared to
210 those of AMF.

211 To be able to better interpret trends results for flood magnitude obtained for
212 different flood series, the Multiple Index (MI) is defined here as:

213 $$MI = Q_F / Q_A \quad (3)$$

214 where Q_F is the mean discharge value of a flood peak series and Q_A is the mean
215 annual discharge recorded for an individual station. Thus, MI indicates how large are
216 the flood peaks in different AMF and POT flood series compared to annual mean flow
217 at each individual station. The MI also indicates for which λ, the POT flood time series
218 represents only larger or combination of larger and smaller flood events.

219

220 **2.3 Trend analysis and test for statistical significance**

221 Trend detection can be performed using parametric or non-parametric approaches.
222 Parametric tests, such as a simple linear regression over time, are useful for the easy
223 representation and interpretation of the trend results (Merz et al. 2012), but need an a-
224 priori assumption on the regression function and require specific statistical
225 characteristics such as normal distribution of the residuals and constant variance (Helsel
226 and Hirsch 2002). If those conditions are not satisfied, non-parametric procedures, such
227 as Mann-Kendall test (Kendall 1938) are preferred. In the present analysis, the Mann-
228 Kendall rank correlation test is adopted for the detection of monotonic trends in flood
229 magnitude and the Theil-Sen-slope algorithm (Sen 1968) is used for a non-parametric
230 trend slope estimation.

231 For the analysis of trends in flood frequency in the POT series, the Chi-squared
232 test of significance on the parametric Poisson regression is used. The Mann-Kendall test
233 has not been applied to the POT-F series, as the presence of several paired values (such
234 as series of counts), the rank correlation procedure may fail in finding a hierarchy in the
235 series (Frei and Schär 2001, Vormoor et al. 2016). The Poisson regression is a
236 generalised linear regression model able to fit count series. The model assumes the
237 counts to be Poisson distributed with the logarithm of their expected value varying
238 linearly with time. The Chi-squared significance test assesses whether the slope
239 parameter of the regression differs significantly from zero, which means that a
240 significant trend in flood frequency is detected. Trends presented in this paper are tested
241 with a two-tailed test at a 10% significance level. For these trends, the corresponding
242 one-tailed tests for the same test statistic is to be considered either twice as significant
243 (half the p-value, 5%), if the trend is in the direction specified by the test (e.g., positive),
244 or not significant at all (p-value above 0.05), if the trend is in the direction opposite that
245 specified by the test (e.g., negative).

246 The presence of autocorrelation within time series is checked here for both the
247 AMF and POT frequency (POT-F) series. In both cases, the Breusch-Godfrey (Breusch
248 1978) test for the presence of serial correlation in time series is used. The test is
249 performed because serially correlated time series tend to “artificially” show higher
250 significance in the trends when trend tests are used (von Storch 1999). Test for serial
251 correlation of the POT magnitude (POT-M) series was not performed, since that would
252 require advanced interpolation methodologies (Rehfeld et al. 2011), which are out of the
253 scope of the present paper.

254

255 **3. Data**

256 ### 3.1 A Pan-European peak discharge dataset

257 The data used in the analysis is based on the 1235 stations listed in the European subset
258 of the Global Runoff Data Centre database (GRDC 2016), recording daily discharge
259 values. The average record length of time series considered is 54 years, the available
260 record length differs considerably between individual stations and possible selected time
261 periods(Fig. 2).

262 In order to maximise both the spatial and temporal coverage of the discharge
263 time series, a common time window of 41 years (1965-2005) is chosen (Fig. 2). Time
264 series with more than 2 years of missing data in the time window are excluded, in order
265 to minimise inhomogeneities within the data, which resulted in 629 gauging stations to
266 be included in the trend analysis.

267 As the aim of this study is to compare the large scale spatial patterns of trends
268 detected in different flood peak series, all time series satisfying the above mentioned
269 criteria are included and no distinction is made between the causes of trends (such as
270 climate, river training or dam construction), as this is outside the scope of this study.

271

272 ### 3.2 Catchment characteristics

273 As this study is also interested in determining the relation between large scale morpho-
274 climatological characteristics of the catchments and significant trends in flood series,
275 the following four catchment characteristics are estimated: catchment area, mean
276 catchment elevation, mean annual rainfall and mean annual air temperature evaluated
277 for the period 1965-2005.

For each catchment the mean elevation is calculated from the European Digital Elevation Model provided by the European Environment Agency (EEA 2016a), with a spatial resolution of 1000 m, while the mean annual precipitation and air temperature are derived from the E-OBS gridded dataset (Haylock et al. 2008). Catchment boundaries for each gauging station have been determined from the Catchment Characterisation and Modelling version 2.1 (CCM2) dataset (Vogt et al. 2007).

The calculated catchment characteristics and the shape files of the catchment boundaries are openly accessible and included in the Supplementary material of this paper.

3.3 Hydro-climatic regions

In order to stratify the results of flood trend detection across Europe, the stations are grouped into five regions: Alpine, Atlantic, Boreal, Continental and Mediterranean regions. The subdivision is based on the biogeographical regions of Europe singled out by the European Environment Agency (EEA 2016b). The hydro-climatic regions are shown in Fig. 3, along with the selected gauging stations, and their description is given in Table 1. The predominant climate of each region is derived from the digital dataset of the Köppen-Geiger climate classification (Köppen 1884, Kottek et al. 2006).

The Alpine region includes the main mountain ranges in Europe: the Alps, the Scandes, the Pyrenees and the Carpathians. Despite their different geographical position, the Alpine region exhibit a number of common features including altitudinal gradients, climatic influence, soil types, geology and vegetation types. The Alps influence the climate of central Europe and divides the Mediterranean region in the south and the temperate region in the north. The Alps are the origin of the many major European rivers such as the Adige, Danube, Po, Rhone and Rhine. About 70 % of the

Alpine region is influenced by human activities (EEA 2002) and the majority of rivers are affected by production of hydro-electric power. The Alpine region encompasses the largest number stations that are included in the analysis.

The Atlantic region is situated along the Atlantic coast and includes Great Britain, Ireland, the Netherlands, the northern shores of Spain and Portugal, and the coastal parts of Germany, Denmark, Belgium and France. The region mainly consists of small hills or flatland and is influenced by an oceanic temperate climate, resulting in relatively mild winters and summers and high rainfall rates throughout the year (EEA 2002). In the region, several large rivers such as the Gironde, Loire, Rhine, Seine, Schelde and Thames drain into the Atlantic Ocean.

The Boreal region covers Estonia and Latvia, South-eastern Norway and most of Sweden, Finland, the northern parts of Lithuania and Belarus and parts of eastern Russia. It is a transition zone between the Arctic and temperate regions of Europe. The climate can be described as cool-temperate mainly sub-continental, with relatively long periods of snow cover (several months) and relatively short growing season (EEA 2002). Most of the region is situated below 500 m a.s.l. Glacial and post-glacial erosion has formed large and undulating plains.

The Continental region covers large areas between Denmark and Sweden in the north and Italy and Balkan region in the south. The region intersects parts of the Alpine region. The climate is continental with strong contrasts between warm summers and cold winters in the central and eastern parts. Precipitation is mainly received during the summer months. In the north, the landscape is flat and becomes increasingly hilly in the south with large flood plains along the large rivers (e.g. the Danube, Desna, Dnepr, Dnestr, Elbe, Loire, Oder, Pripyat, Rhine, Vistula or Volga) (EEA 2002).

The Mediterranean region is situated between the Atlantic region in the west and the Continental and Alpine regions in the north. The climate is dry and warm, with hot summers and mild winters. Hills and mountains dominate the landscape, with the low mountain ranges being intersected by inland plateaus. In the Mediterranean region, there is a pronounced variability in climate and topographic characteristics due to a variety of small scale landscape characteristics such as slope, exposition, geology and the distance to the sea (EEA 2002). The largest rivers draining into the Mediterranean Sea are the Adige, Drin-Bojana, Ebro, Neretva, , Rhone and Tiber. This region contains the smallest number of gauging stations.

4. Results

4.1 Frequency of discharge peak events

Fig. 4 shows the spatial pattern of the mean number of independent discharge peak events per year, identified according to the procedure presented in the section 2.1. The panels around the map give typical two-year example of the variability of different runoff hydrographs across the five hydro-climatic regions.

Fig. 5 summarises the results of the discharge peaks identification based on the five regions and shows the variability of the mean number of independent peaks per year identified across Europe.

The highest number of peaks is observed in the Atlantic and Alpine region, with a median value of ~ 16 events per year. In the Atlantic region, 10% of stations exhibit a mean number of peaks per year larger than 30, most of which are situated in northern England and Scotland (Fig. 4). A lower median mean number of peaks per year (14) is found in the Continental region the median, as well as the upper 10 percentile (16).

In the Boreal and Mediterranean region, the median mean number of peaks per year is the lowest. In particular, in the Boreal region, snow accumulation and melting processes dominates the runoff regime, resulting in the smallest number of peaks. In this region, not more than a mean of five peaks per year can be identified in many catchments. In the arid Mediterranean region, the variability of the mean number of peaks per year within a region is the lowest (Fig. 5). The median mean number of peaks events in this region is 10 independent events per year.

4.2 Trends in AMF and POT1 series

The results of trend detection in Annual Maximum Flood series (AMF) are presented in Fig. 6. Significant positive and negative trends in AMF series are detected at 61 (10%) and 48 (8%) stations respectively, both at a 5% significance level, whereas the other 520 stations show no evidence of a significant trend. This means that, when considering the whole dataset, the number of detected significant trends are more than what could be expected by chance. Moreover, large-scale spatially coherent patterns of trends with the same direction can be identified. These trend patterns are of practical importance and indicate the possibility of common drivers. Therefore, a description of the trends found in the individual regions is given below. The largest number of stations (23) exhibiting significant positive trends in AMF series is found in the Atlantic region (21 stations in Great Britain and two in the western France), while only six stations (three in England and three smaller catchments in southern France) exhibits significant negative trends in the same region.

A large number of stations exhibiting either significant increasing (16 stations) or decreasing (13 stations) trends in AMF series is detected in the Continental region.

374 Increasing trends are observed in the eastern France, in the upper Danube and in three
375 large catchments in Central Germany (Lahn, Neckar and Rhine rivers). Decreasing
376 trends are observed in large catchments (Schwarze Elster, Havel and Oder River) in the
377 eastern Germany and few small catchments in southern France.

378 Significant decreasing trends are mostly detected in the Alpine region (19
379 stations). These catchments are located in the south-eastern France (near the border with
380 Switzerland) and southward of the main ridge of Central Alps in Austria and Tatra
381 Mountains in Slovakia. Increasing flood trends in Alpine region tend to be detected in
382 small catchments, having mean catchment area of about 200 km^2. These catchments are
383 located in central Switzerland, Tirol and southern Bavaria.

384 In the Boreal region, four and seven stations show increasing or decreasing
385 trends, respectively. While increasing flood trends are detected in two catchments in
386 Finland and two catchments in southern Sweden, negative trends are detected in three
387 small catchments (catchment area smaller than 10 km^2) located in the southern part of
388 Sweden and four larger catchments in Southern Finland and Eastern Sweden.

389 In the Mediterranean region, no clear pattern of flood trends can be found: three
390 catchments exhibit increasing flood trends but also three stations with decreasing flood
391 trends are found.

392 Interestingly, stations exhibiting significant changes in AMF series present a
393 mean number of peaks per year very close to the median mean values of each individual
394 regional distributions. Exceptions are the catchments exhibiting trends in the Atlantic
395 region, in which the mean numbers of peaks per year belong to the upper part of the
396 regional distribution.

397 The trend analysis on Peak Over Threshold (POT) series is presented next in
398 Fig. 7, which shows the results of setting the threshold λ a mean of 1 events per year
399 (POT1), with respect to trends in flood magnitude (POT1-M, left panel) and trends in
400 flood frequency (POT1-F, right panel).

401 The left panel of Fig. 7 shows the spatial pattern of flood change detected in the
402 POT1-M series. The total number of stations exhibiting significant trends in POT1-M
403 series is slightly lower than the number of stations exhibiting trends in AMF series. The
404 AMF (exactly one flood event per year) and POT1 (an average of one event per year)
405 series can be compared, given the same sample size and 5% significance level of the
406 one-sided tests. Interestingly, trends in POT1-M series and AMF series are not always
407 detected in the same catchments, which results in a different spatial pattern of flood
408 change in the two cases.

409 Significant positive or negative trends in POT1-M series are detected in 57 (9%)
410 and 40 (6%) stations, respectively. Similarly to the trends detected in AMF, the number
411 of detected trends are more than what could be expected by chance, when considering
412 the whole dataset. Also in the case of POT1, spatially coherent patterns of trend can be
413 found. The majority of catchments with increasing trends is situated in the Continental
414 (31 stations, mostly in Germany) and Alpine (16 stations, situated mostly in Bavaria and
415 Tirol) region. Only eight catchments in the Atlantic region exhibit increasing trends in
416 POT1-M series, a relatively small number compared to the significant trends detected in
417 AMF series.

418 Significant negative trends in POT1-M series are detected in 19 catchments in
419 the Boreal region (Scandinavia), which is almost three times more than what is detected
420 in AMF series. Moreover, less negative trends in POT1-M series are detected (10
421 stations) in the Alpine region (southern Austria, Slovenia) compared to AMF series.

422 Significant trends in POT1-F series (Fig.7, right panel) are detected in 133 stations. In
423 particular, an increasing trend in POT1-F series is detected in 68 (11%) stations, and a
424 decreasing trend in 65 (10%) stations. This would suggest that the trends in frequency
425 are significant for Europe as a whole. Again, when considering the hydro-climatic
426 regions independently discernible spatial patterns emerge. The highest number of the
427 catchments exhibiting either positive or negative trends in POT1-F series are situated in
428 the Atlantic region (29 stations in Great Britain out of 37 in the region) and in the
429 Alpine region (35 stations, mostly in Central and East Alps, Slovenia and rivers
430 originating in Tatra Mountains in Slovakia), respectively.

431

432 **4.3 Sensitivity of flood trends to the selection of different flood series**

433 The trends in flood magnitude in the AMF and POT1-M series (Fig. 6 and 7) indicated
434 different spatial patterns of flood changes across Europe. The next section in this paper
435 investigates the sensitivity of trends in POT series with regard to the selection of
436 different exceedance thresholds λ.

437 Generally, different exceedance thresholds imply an increasing number of flood
438 peaks considered for increasing λ. While POT1-M series represent a compilation of the
439 largest floods recorded at each gauging station, an increase in λ determines a lower
440 threshold and therefore an increase in the number of (smaller) events considered.

441 Fig. 8 shows the variability of the Multiple Index (MI), the ratio between the
442 mean discharge magnitude of the flood series and the mean annual discharge for
443 individual stations, estimated for the AMF and the different POT-M flood series in the
444 five hydro-climatic regions. The MI of the POT1-M series is the largest, while results

445 indicate that the MI of the AMF series tends to be slightly bigger than the MI of the
446 POT2-M series in all the regions. The smallest MI is estimated in POT6-M flood series.

447 The median value of the MI in POT1-M series ranges between four (i.e. 4 times
448 the mean annual flow) in the Boreal region to more than 23 in the Mediterranean region.
449 This result can be explained by the different hydrological flood regimes across Europe.
450 On one side, the arid climate of the Mediterranean region implies a dry mean discharge
451 regime during the year that is offset by intense precipitation events leading to extreme
452 values. Moreover, the subset of stations in the Mediterranean region considered here is
453 mainly composed of small catchments, which have an intrinsically high variance in the
454 hydrograph. On the other side, snowmelt processes drive the extreme values in the
455 Boreal region. In this case, the volume of the peak is large but the maximum intensity
456 reached remains in the order of magnitude of the mean discharge regime.

457 The sensitivity of trends in POT series to the selection of different exceedance
458 thresholds λ is assessed for a mean number of floods per year ranging from 1 to 6 (i.e.
459 POT1 to POT6). Table 2 and 3 present the absolute number of trends detected in the
460 flood series in each regions.

461 Similarly, Fig. 9 shows the percentage of stations exhibiting significant positive
462 or negative trends, both tested at 10% significance level, for the six different
463 exceedance thresholds, grouping the stations into the five hydro-climatological regions.

464 The almost horizontal lines in Figure 9 suggest that results of trend analyses in POT
465 series are not very sensitive to the selection of the threshold, with the exception of
466 trends in flood frequency in the Mediterranean and Boreal region. In particular, with
467 increasing the mean number of events per year λ, a greater amount of significant
468 negative trends in flood frequency are detected in the Western part of the Mediterranean

469 region (i.e. Southern France), while significant positive trends increase in number in the
470 Boreal catchments situated on the coast.

471 Top panel of Fig. 9 shows the percentage of significant increasing and
472 decreasing trends in POT1-M to POT6-M series. The percent number of stations
473 exhibiting significant trends and the general regional tendency differs significantly
474 between the regions.

475 In the Alpine and Boreal regions, decreasing trends dominate, with exception for
476 the POT1-M series in the Alpine region. The largest number of stations exhibiting
477 decreasing trends in the Alpine region is observed in POT6-M series, while the Boreal
478 region exhibits the most relevant negative trends in the floods series containing the
479 highest peaks (POT1-M).

480 The general tendency in the Atlantic region is the opposite, except for the POT1-
481 M series, significant increasing trends are observed in POT2 to POT6 series at more
482 than 15% of stations.

483 In the Continental region, the highest percentage of positive trends is detected in
484 POT1-M series while, considering higher λ thresholds, the number of stations exhibiting
485 significant trends is smaller and the general tendency differs. However, from POT1-M
486 to POT4-M series, positive trends dominate. When including smaller floods in POT5-M
487 and POT6-M series, a larger number of stations exhibit decreasing trends is found.

488 In the Mediterranean region, a prevailing tendency towards increasing flood
489 magnitude is found, but the number of stations included in the region is rather small to
490 be able to draw general conclusions.

491 Bottom panel of Fig. 9 shows the significant trends detected in POT-F series. A
492 clear tendency towards increasing flood frequency is found in the Atlantic, which is
493 even more evident when considering lower λ values (POT1-F or POT2-F series).

494 Significant negative trends in flood frequency are detected in the Continental
495 and Alpine region, where decreasing trends are much more apparent in all series when
496 compared to the trends in flood magnitude for the same regions.

497 Significant positive trends in flood frequency are found in the Boreal region and
498 the percentage of stations exhibiting this tendency increases for increasing λ. From
499 POT3-F to POT6-F series, the increase in flood frequency is observed in more than one
500 station out of three. Interestingly, only a very small number of catchments exhibits
501 concurrent significant trends in both flood frequency and magnitude.

502 An opposite pattern compared to the Boreal region is found in the Mediterranean
503 region, where a higher percentage of significant decreasing trends are detected for
504 increasing λ.

505 While significant trends can be regionally considered not very sensitive to the
506 selection of the threshold (apart for the cases analysed above), trends detected at
507 individual stations may considerably change over the different flood series.

508 Fig. 10 and 11 summarise, for each individual station, the results of trends
509 detected in flood magnitude (comparing AMF and POT-M) series and frequency
510 (considering only POT-F series), respectively. The diverging colour scale indicates the
511 intensity of the decadal change (% per decade) detected in the different flood series.
512 Negative trends are depicted with yellow to red colours and positive trends with light to
513 dark blue colours. Only those stations that exhibit a significant trend (at 10%

514 significance level) in at least one of the different flood series are presented in the
515 figures.

516 Considering trends in flood magnitude (Fig. 10), between 33% of the stations (in
517 the Atlantic region) and 45% of the stations (in the Boreal region) exhibit trends in at
518 least two different flood series. An exception is the Continental region, where only 21%
519 of the stations exhibit trends in at least two different flood series. If a stricter criterion is
520 used, around 15% of the stations in total exhibits consistent trends in at least three
521 different flood series.

522 Results differ when considering trends in flood frequency (Fig. 11). In this case,
523 a much more consistent situation is visible over the different thresholds considered:
524 more than 30% of the stations in almost all the regions in Europe exhibit trends in at
525 least three different flood series.

526 AMF series exhibit the largest intensity of decadal change in flood magnitude,
527 with median values of 9% or 10% per decade for increasing or decreasing trends,
528 respectively. The median intensity of decadal change in POT1-M series is 5% per
529 decade for increasing trends and 4% per decade for decreasing trends, while lower
530 median intensities are detected in the other POT-M series (POT2-M to POT6-M).

531 The magnitude of changes in flood frequency is small and decreases
532 significantly with increasing exceedance threshold, with similar values for increasing
533 and decreasing trends. The median intensity of change in POT1-F series is 0.3 event per
534 decade and decreases to less than 0.14 events per decade in POT6-F series.

535 Interestingly, both for trends in magnitude and frequency, no inversions in sign
536 of significant trends detected with different thresholds are found out.

537 In order to test the sensitivity of the results to the representativeness of coverage
538 of stations and to the issue of sites with human interventions, all analyses above have
539 been repeated in two cases: (1) by removing randomly all sites with the same river name
540 but one (i.e., removing 22% of the sites); (2) by removing all sites for which a step
541 change in the time series of runoff flashiness, quantified by the ratio of absolute day-to-
542 day fluctuations of streamflow relative to total flow in a year (see Holko et al., 2011),
543 has not been detected by the Pettitt test at the 10% significance level (i.e., removing
544 41% of the sites). In both cases, essentially the same conclusions have been obtained as
545 those showed here (see Supplementary material Figures S1 and S2 for a comparison
546 with Figure 9).

547 **4.4 Physiographic characteristics of catchments exhibiting significant changes**
548 **in flood magnitude and frequency**

549 Fig. 12 shows the distribution of the mean elevation (top left panel), area (top right
550 panel), mean annual precipitation (bottom left panel) and mean annual air temperature
551 (bottom right panel) of those catchments which exhibit significant increasing or
552 decreasing trends in flood magnitude. Categories along x-axes indicate the different
553 flood series considered: AMF and POT1-M to POT6-M series.

554 Results indicate that the significantly increasing trends in flood magnitudes
555 detected in AMF series and POT-M series selected by high mean number of exceedance
556 per year λ (i.e. POT3-M, POT5-M and POT6-M) tend to occur more often in low-
557 elevation watersheds, with mean elevation below 400 m asl. The flood series of the
558 largest floods (POT1-M) have an opposite tendency, which is decreasing flood
559 magnitude in catchments having low mean elevation. However, there is a clear tendency
560 towards increasing flood magnitudes in catchments having a high mean annual air

561 temperature and high mean annual precipitation rates. Conversely, a relationship
562 between catchment size and significant trends cannot be seen.

563 Fig. 13 shows a clear pattern of increasing flood frequency in catchments with
564 low mean catchment elevation and low mean annual air temperature, particularly for
565 POT2 and higher λs. These catchments are also characterised by a lower mean annual
566 precipitation, when compared to catchments exhibiting decreasing trends in flood
567 frequency. Again, no clear relationship between the size of catchments and the detected
568 trends can be found.

569

570

5. Discussion and conclusions

The overall aim of this study is to contribute to the detection of flood trends in Europe. Compared to previous works, three novel aspects have been investigated. First, the comparison of two different methods used to derive flood series at the European scale: the Annual Maximum Flood (AMF) and the Peak Over Threshold (POT) approach. Second, the sensitivity analysis of flood trends with respect to different exceedance thresholds in the POT approach. Third, the full reproducibility of the analyses is given, supporting the value of open data and tools for the advance of hydrological science.

Previous regional or continental studies in Europe have analysed the spatial pattern of flood trends either in predefined regions, as discussed by Kundzewicz (2012) and Hall et al. (2014), or in regions exhibiting similar flood regime based on clustering techniques (Parajka et al. 2010, Mediero et al. 2015). In this study, regional patterns are analysed in predefined regions based on a biogeographical classification of Europe (EEA 2016b). The Alpine, Atlantic, Boreal, Continental and Mediterranean regions used here to stratify the trend results correspond approximately to the three main regions (Atlantic western Europe and northern Europe, Continental central Europe and eastern Europe, and the European Mediterranean) identified in Hall et al. (2014) or with the five regions derived from cluster analysis presented by Mediero et al. (2015) which allows a comparison of the results cross these papers.

When considering Europe as a whole, the percent of stations with statistically significant trends (10% significance level for the two-sided tests, 5% level for the one-sided tests), across all types of flood series, is more than what would be expected by chance alone. Moreover, coherent larger-scale spatial patterns of significant trends can be identified across the European continent for different series of flood peaks. For example, a general tendency towards increasing flood magnitude and frequency is found

596 in Atlantic region. The flood magnitude increases more in AMF series and POT-M
597 series selected by lower exceedance threshold λ. A significant increase in flood
598 magnitude in flood series with high peaks (i.e. POT1-M, POT2-M) is only detected in
599 few stations, but trends in flood frequency are more apparent when considering the
600 same thresholds (i.e. POT1-F, POT2-F). The increasing trends detected in AMF are
601 consistent with the main findings of Hannaford and Buys (2012) and Murphy et al.
602 (2013) for England and Ireland, respectively, but for slightly different time periods.

603 In the Boreal region, a clear tendency towards increasing flood frequency and
604 decreasing flood magnitude is detected in POT series. This is in line with the main
605 findings presented in Hall et al. (2014), for the northern part of Eastern Europe and
606 Scandinavia. Differently, no apparent pattern of change in flood magnitude is detected
607 when considering AMF series (Fig. 6). Similar conclusions were also drawn by
608 Arheimer and Lindström (2015) for Swedish catchments, in which the authors detected
609 no widespread evidence of flood trends in 69 AMF series.

610 The Central region presents the highest percentage of stations (17%) exhibiting
611 significant positive trends in magnitude in the POT1-M series. Similarly, Kundzewicz et
612 al. (2013) found that positive trends can be detected in that region with respect to two
613 metrics (flood severity, related to flood frequency, and flood magnitude) when
614 analysing the main flood events over the time period 1985–2009. However, when
615 lowering the threshold λ, a higher number of decreasing trends in flood magnitude and
616 frequency can be detected, especially on the Elbe River. This is in accordance with the
617 negative trends detected in Brázdil et al. (2006, 2012) within the Czech Republic
618 boundaries.

619 The Alpine region, including the Alps and other main mountain areas of Europe,
620 exhibits similar pattern of flood changes as described in Blöschl et al. (2011) for the

621 Austrian parts of the Alps. In the northern part of the main alpine ridge, a general
622 tendency for increasing flood trends is detected, while a clear pattern towards
623 decreasing flood magnitude is detected in the southern part of the Alps, particularly for
624 POT series compiled by high λ values (i.e. considering smaller floods). Similar pattern
625 of decreasing flood magnitude are found here in south-eastern France and in the alpine
626 rivers originating in Tatra Mountains. Pattern of flood trends in the POT3 series indicate
627 similar decreasing tendencies, as shown by Mediero et al. (2015).

628 The Mediterranean region shows a general tendency towards increasing flood
629 magnitude and decreasing flood frequency, especially in series compiled by lower λ.
630 This is in line with results presented in Giuntoli et al. (2012) in French.

631 From a methodological point of view, this study shows that the number of
632 catchments exhibiting significant changes within a region is consistent over the different
633 thresholds (Fig. 9), with a few exception (such as trends in flood frequency in the
634 Mediterranean and Boreal regions). The detection of trends in flood magnitude and the
635 frequency from POT series is an alternative to AMF approach and indicates regionally
636 consistent trends over the different thresholds. Fig. 10 and 11 show, however, that the
637 number of catchments exhibiting significant changes for a large range of exceedance
638 threshold (> 3 threshold) is rather small, particularly when analysing trends in flood
639 magnitude. Overall, the results show a larger number of stations exhibiting significant
640 changes in flood frequency than in flood magnitude.

641 Thus, in Europe, similar to the trend analysis of Archfield et al. (2016) in the
642 US, the picture of flood change obtained is strongly heterogeneous and no general
643 statements of uniform trends across the entire continent can be detected, but regional
644 pattern exist.

The regions with consistent spatial patterns of significant trends across the different flood series identified here show that the trends detected can be considered real and not an artefact of the method used to derive the series. Such areas can serve as prime locations for future studies aiming to attribute the trends not only for individual catchments but rather attributing changes with methods that allow for a regional scale assessment such as the scaling fingerprints (Viglione et al., 2016).

Finally, data, tools and results used in the study are openly accessible. In the supplement material, a table listing the station name, geographical coordinates, selected physiographic attributes and the results of trend detection is provided (data access at: http://www.water-switch-on.eu/sip-webclient/byod/#/resource/12069). Daily runoff time series can be obtained from the Global Runoff Data Centre on request, while the derived catalogue of flood peak events can be accessed under the name of "Pan-European catalogue of flood events" in the Spatial Information Platform of the SWITCH-ON portal (data access at http://www.water-switch-on.eu/sip-webclient/byod/#/resource/12056). Following the recommendation of Ceola et al. (2015), the authors believe that the availability of all data, tools and results will allow further advancing the research concerning flood change, as it will facilitate comparison and extension of the current study. Future studies could for example further investigate the controlling factors of flood trends or attribute the spatial patterns of the detected trends to possible drivers.

Acknowledgements

This study was performed within the EU FP7-funded project SWITCH-ON [grant numbers 603587, 2014], which explores the potential of Open Data for comparative hydrology and collaborative research, as well as promote Open Science for transparency and reproducibility. All data, scripts and protocols are available in the SWITCH-ON Virtual Water-Science Laboratory at www.water-switch-on.eu for review.

The work was supported by the ERC Advanced Grant "FloodChange" [number 291152, 2011] and the MSCA-ITN-ETN SYSTEM RISK [numbers 676027, 2015].

Finally, the authors acknowledge the E-OBS dataset from the EU-FP6 project ENSEMBLES (http://ensembles-eu.metoffice.com), the data providers in the ECA&D project (http://www.ecad.eu), the Global Runoff Data Centre, 56068 Koblenz, Germany and the CCM River and Catchment Database © European Commission - JRC, 2007 for the data.

The paper was developed using Copernicus data and information funded by the European Union - EU-DEM layers.

681

682 **References**

683 Archfield, S.A., Hirsch, R.M., Viglione, A., Blöschl, G., 2016. Fragmented patterns of flood
684 change across the United States. *Geophysical Research Letters* **10**, 232–239.
685 doi:10.1002/2016GL070590.

686 Arheimer, B., Lindström, G., 2015. Climate impact on floods: changes in high flows in Sweden
687 in the past and the future (1911-2100). *Hydrology and Earth System Sciences* **19**, 771–784.
688 doi:10.5194/hess-19-771-2015.

689 Bard, A., Renard, B., Lang, M., 2012. Floods in the Alpine Areas of Europe, in: Zbigniew W.
690 Kundzewicz (Ed.), Changes in Flood Risk in Europe. *IAHS Press and CRC Press/Balkema*,
691 Wallingford, UK, 375–384.

692 Blöschl, G., Nester, T., Komma, J., Parajka, J., Perdigão, R.A.P., 2013. The June 2013 flood in
693 the Upper Danube Basin, and comparisons with the 2002, 1954 and 1899 floods. *Hydrology and*
694 *Earth System Sciences* **17**, 5197–5212. doi:10.5194/hess-17-5197-2013.

695 Blöschl, G., Viglione, A., Merz, R., Parajka, J., Salinas, L.J., Schöner, W., 2011. Climate
696 impacts on floods and low flows. *Österreichische Wasser- und Abfallwirtschaft* **63**, 21–30.
697 doi:10.1007/s00506-010-0269-z.

698 Brázdil, R., Dobrovolný, P., Kakos, V., Kotyza, O., 2006. Historical and recent floods in the
699 Czech Republic: causes, seasonality, trends, impacts, in: Flood Risk Management: Hazards,
700 Vulnerability and Mitigation Measures. *Springer*, Dordrecht, 247–259.

701 Brázdil, R., Reznickova, L., Havlicek, M., Elleder, L., 2012. Floods in the Czech Republic, in:
702 Zbigniew W. Kundzewicz (Ed.), Changes in Flood Risk in Europe. *IAHS Press and CRC*
703 *Press/Balkema*, Wallingford, UK, 191–211.

704 Breusch, T.S., 1978. Testing for autocorrelation in dynamic linear models. *Australian Economic*
705 *Papers* **17**, 334–355. doi:10.1111/j.1467-8454.1978.tb00635.x.

706 Ceola, S., Arheimer, B., Baratti, E., Blöschl, G., Capell, R., Castellarin, A., Freer, J., Han, D.,
707 Hrachowitz, M., Hundecha, Y., Hutton, C., Lindstr□m, G., Montanari, A., Nijzink, R., Parajka,
708 J., Toth, E., Viglione, A., Wagener, T., 2015. Virtual laboratories: new opportunities for
709 collaborative water science. *Hydrology and Earth System Sciences* **19**, 2101–2117.
710 doi:10.5194/hess-19-2101-2015.

711 Chapman, T., 1999. A comparison of algorithms for stream flow recession and baseflow
712 separation. *Hydrological Processes* **13**, 701–714. doi:10.1002/(SICI)1099-
713 1085(19990415)13:5<701::AID-HYP774>3.0.CO;2-2.

714 Cunnane, C., 1973. A particular comparison of annual maxima and partial duration series
715 methods of flood frequency prediction. *Journal of Hydrology* **18**, 257 – 271. doi:10.1016/0022-
716 1694(73)90051-6.

717 EEA, 2002. Biogeographical regions in Europe [online]. *EEA Report No 1/2002*. Available
718 from: http://www.eea.europa.eu/publications/report_2002_0524_154909.

719 EEA, 2016a. Digital Elevation Model over Europe [online]. Available from:
720 http://www.eea.europa.eu/data-and-maps/data/eu-dem.

721 EEA, 2016b. Biogeographical regions [online]. Available from: http://www.eea.europa.eu/data-
722 and-maps/data/biogeographical-regions-europe-3#tab-gis-data.

723 Frei, C., Schär, C., 2001. Detection Probability of Trends in Rare Events: Theory and
724 Application to Heavy Precipitation in the Alpine Region. *Journal of Climate* **14**, 1568–1584.
725 doi:10.1175/1520-0442(2001)014<1568:DPOTIR>2.0.CO;2.

726 Giuntoli, I., Renard, B., Lang, M., 2012. Floods in France, in: Zbigniew W. Kundzewicz (Ed.),
727 Changes in Flood Risk in Europe. *IAHS Press and CRC Press/Balkema*, Wallingford, UK, 212–
728 224.

729 GRDC, 2016. The Global Runoff Data Centre [online]. Available from:
730 http://www.bafg.de/GRDC/EN/Home/homepage_node.html.

731 Gumbel, E.J., 1958. Statistics of extremes, ISBN 0-486-43604-7. ed. *Columbia University*
732 *Press*, New York.

733 Hall, J., Arheimer, B., Borga, M., Brázdil, R., Claps, P., Kiss, A., Kjeldsen, T.R.,
734 Kriauvcianiena, J., Kundzewicz, Z.W., Lang, M., Llasat, M.C., Macdonald, N., McIntyre, N.,
735 Mediero, L., Merz, B., Merz, R., Molnar, P., Montanari, A., Neuhold, C., Parajka, J., Perdigão,
736 R.A.P., Plavcová, L., Rogger, M., Salinas, J.L., Sauquet, E., Schär, C., Szolgay, J., Viglione, A.,
737 Blöschl, G., 2014. Understanding flood regime changes in Europe: a state-of-the-art assessment.
738 *Hydrology and Earth System Sciences* **18**, 2735–2772. doi:10.5194/hess-18-2735-2014.

739 Hannaford, J., Buys, G., 2012. Trends in seasonal river flow regimes in the UK. *Journal of*
740 *Hydrology* **475**, 158 – 174. doi:10.1016/j.jhydrol.2012.09.044.

741 Haylock, M.R., Hofstra, N., Klein Tank, A.M.G., Klok, E.J., Jones, P.D., New, M., 2008. A
742 European daily high-resolution gridded data set of surface temperature and precipitation for
743 1950–2006. *Journal of Geophysical Research: Atmospheres* **113**, D20119.
744 doi:10.1029/2008JD010201.

745 Helsel, D.R., Hirsch, R.M., 2002. Statistical Methods in Water Resources Techniques of Water
746 Resources Investigations. *U.S. Geological Survey*.

747 Hirsch, R.M., Archfield, S.A., 2015. Flood trends: Not higher but more often. *Nature climate*
748 *change* **5**, 198–199. doi:10.1038/nclimate2551.

749 Jeneiová, K., Kohnová, S., Hall, J., Parajka, J. (2016) Variability of seasonal floods in the
750 Upper Danube River basin, J. Hydrol. Hydromech., Vol. 64, No. 4, 2016, p. 357 – 366 , doi:
751 10.1515/johh-2016-0037.

752 Kendall, M.G., 1938. A New Measure of Rank Correlation. *Biometrika* **30**, 81–93.

753 Khaliq, M.N., Ouarda, T.B.M.J., Ondo, J.-C., Gachon, P., Bobée, B., 2006. Frequency analysis
754 of a sequence of dependent and/or non-stationary hydro-meteorological observations: A review.
755 *Journal of Hydrology* **329**, 534–552. doi:10.1016/j.jhydrol.2006.03.004.

Köppen, W., 1884. Die Waermezonen der Erde, nach der Dauer der heissen, gemaessigten und kalten Zeit und nach der Wirkung der Waerme auf die organische Welt betrachtet (The thermal zones of the Earth according to the duration of hot, moderate and cold periods and to the impact of heat on the organic world). *Meteorologische Zeitschrift* **1**, 215–226. doi:10.1127/0941-2948/2011/105.

Kottek, M., Grieser, J., Beck, C., Rudolf, B., Rubel, F., 2006. World Map of the Köppen-Geiger climate classification updated. *Meteorologische Zeitschrift* **15**, 259–263. doi:10.1127/0941-2948/2006/0130.

Kundzewicz, Z., 2012. Changes in flood risk in Europe. *IAHS Press Wallingford*.

Kundzewicz, Z.W., Pińskwar, I., Brakenridge, G.R., 2013. Large floods in Europe, 1985–2009. *Hydrological Sciences Journal* **58**, 1–7. doi:10.1080/02626667.2012.745082.

Lang, M., Ouarda, T.B.M.J., Bobée, B., 1999. Towards operational guidelines for over-threshold modeling. *Journal of Hydrology* **225**, 103–117. doi:S0022-169499001675.

Madsen, H., Rasmussen, P.F., Rosbjerg, D., 1997. Comparison of annual maximum series and partial duration series methods for modeling extreme hydrologic events: 1. At-site modeling. *Water Resources Research* **33**, 747–757. doi:10.1029/96WR03848.

Mallakpour, I., Villarini, G., 2015. The changing nature of flooding across the central United States. *Nature Climate Change* **5**, 250–254. doi:10.1038/nclimate2516.

Marchi, L., Boni, G., Cavalli, M., Comiti, F., Crema, S., Lucia, A., Marra, F., Zoccatelli, D., 2013. The flash flood of October 2011 in the Magra River basin (Italy): rainstorm characterisation and flood response analysis. *Geophysical Research Abstracts* **15**, EGU2013-11125.

Marsh, T., 2008. A hydrological overview of the summer 2007 floods in England and Wales. *Weather* **63**, 274–279. doi:10.1002/wea.305.

780 Mediero, L., Kjeldsen, T.R., Macdonald, N., Kohnova, S., Merz, B., Vorogushyn, S., Wilson,
781 D., Alburquerque, T., Blöschl, G., Bogdanowicz, E., Castellarin, A., Hall, J., Kobold, M.,
782 Kriauciuniene, J., Lang, M., Madsen, H., Gül, G.O., Perdigão, R.A.P., Roald, L.A., Salinas,
783 J.L., Toumazis, A.D., Veijalainen, N., Þórarinsson, Ó., 2015. Identification of coherent flood
784 regions across Europe by using the longest streamflow records. *Journal of Hydrology* **528**, 341
785 – 360. doi:10.1016/j.jhydrol.2015.06.016.

786 Méndez, F.J., Menéndez, M., Luceño, A., Losada, I.J., 2006. Estimation of the long-term
787 variability of extreme significant wave height using a time-dependent Peak Over Threshold
788 (POT) model. *Journal of Geophysical Research: Oceans* **111**. doi:10.1029/2005JC003344.

789 Merz, B., Kundzewicz, Z.W., Delgado, J., Hundecha, Y., Kreibich, H., 2012. Detection and
790 Attribution of Changes in, in: Zbigniew W. Kundzewicz (Ed.), Changes in Flood Risk in
791 Europe. *IAHS Press and CRC Press/Balkema*, Wallingford, UK, 446–469.

792 Muchan, K., Lewis, M., Hannaford, J., Parry, S., 2015. The winter storms of 2013/2014 in the
793 UK: hydrological responses and impacts. *Weather* **70**, 55–61. doi:10.1002/wea.2469.

794 Murphy, C., Harrigan, S., Hall, J., Wilby, R.L., 2013. Climate-driven trends in mean and high
795 flows from a network of reference stations in Ireland. *Hydrological Sciences Journal* **58**, 755–
796 772. doi:10.1080/02626667.2013.782407.

797 Parajka, J., Kohnová, S., Bálint, G., Barbuc, M., Borga, M., Claps, P., Cheval, S., Dumitrescu,
798 A., Gaume, E., Hlavčová, K., Merz, R., Pfaundler, M., Stancalie, G., Szolgay, J., Blöschl, G.,
799 2010. Seasonal characteristics of flood regimes across the Alpine–Carpathian range. *Journal of*
800 *Hydrology* **394**, 78–89. doi:10.1016/j.jhydrol.2010.05.015.

801 Parry, M.L., Canziani, O.F., Palutikof, J.P., van der Linden, P.J., Hanson, C.E., 2007. IPCC,
802 2007. Climate change 2007: impacts, adaptation and vulnerability. *Contribution of working*
803 *group II to the fourth assessment report of the intergovernmental panel on climate change.*

804 Pekárová, P., Pramuk, B., Halmová, D., Miklánek, P., Prohaska, S., Pekár, J., 2016.
805 Identification of long-term high-flow regime changes in selected stations along the Danube
806 River. *Journal of Hydrology and Hydromechanics* **64**, 393–403.

807 Petrow, T., Merz, B., 2009. Trends in flood magnitude, frequency and seasonality in Germany
808 in the period 1951–2002. *Journal of Hydrology* **371**, 129–141.
809 doi:10.1016/j.jhydrol.2009.03.024.

810 Rehfeld, K., Marwan, N., Heitzig, J., Kurths, J., 2011. Comparison of correlation analysis
811 techniques for irregularly sampled time series. *Nonlinear Processes in Geophysics* **18**, 389–404.
812 doi:10.5194/npg-18-389-2011.

813 Renard, B., Lang, M., Bois, P., 2006. Statistical analysis of extreme events in a non-stationary
814 context via a Bayesian framework: case study with peak-over-threshold data. *Stochastic*
815 *Environmental Research and Risk Assessment* **21**, 97–112. doi:10.1007/s00477-006-0047-4.

816 Rosner, A., Vogel, R.M., Kirshen, P.H., 2014. A risk-based approach to flood management
817 decisions in a nonstationary world. *Water Resources Research* **50**, 1928–1942.
818 doi:10.1002/2013WR014561.

819 Schröter, K., Kunz, M., Elmer, F., Mühr, B., Merz, B., 2015. What made the June 2013 flood in
820 Germany an exceptional event? A hydro-meteorological evaluation. *Hydrology and Earth*
821 *System Sciences* **19**, 309–327. doi:10.5194/hess-19-309-2015.

822 Sen, P.K., 1968. Estimates of the Regression Coefficient Based on Kendall's Tau. *Journal of the*
823 *American Statistical Association* **63**, 1379–1389. doi:10.2307/2285891.

824 Šraj, M., Viglione, A., Parajka, J., Blöschl, G., 2016. The influence of non-stationarity in
825 extreme hydrological events on flood. *Journal of Hydrology and Hydromechanics* **64**(4), 426–
826 437. doi:10.1515/johh-2016-0032.

827 Svensson, C., Kundzewicz, W.Z., Maurer, T., 2005. Trend detection in river flow series: 2.
828 Flood and low-flow index series. *Hydrological Sciences Journal* **50**, 811–824.
829 doi:10.1623/hysj.2005.50.5.811.

830 Thomas, B.F., Vogel, R.M., Kroll, C.N., Famiglietti, J.S., 2013. Estimation of the base flow
831 recession constant under human interference. *Water Resources Research* **49**, 7366–7379.
832 doi:10.1002/wrcr.20532.

833 Ulbrich, U., Brücher, T., Fink, A.H., Leckebusch, G.C., Krüger, A., Pinto, J.G., 2003. The
834 central European floods of August 2002: Part 1 – Rainfall periods and flood development.
835 *Weather* **58**, 371–377. doi:10.1256/wea.61.03A.

836 USWRC, 1982. Guidelines for determining flood flow frequency, Bulletin #17B. ed.
837 Interagency Advisory Committee on Water Data. water.usgs.gov/osw/bulletin17b/dl_flow.pdf.

838 Viglione, A., Merz, B., Viet Dung, N., Parajka, J., Nester, T., & Blöschl, G. (2016). Attribution
839 of regional flood changes based on scaling fingerprints. *Water Resources Research*, **52**(7),
840 5322-5340, doi:10.1002/2016WR019036.

841 Vogel, R.M., Kroll, C.N., 1996. Estimation of baseflow recession constants. *Water Resources*
842 *Management* **10**, 303–320.

843 Vogel, R.M., Yaindl, C., Walter, M., 2011. Nonstationarity: Flood magnification and recurrence
844 reduction factors in the United States. *Journal of the American Water Resources Association* **47**,
845 464–474. doi:10.1111/j.1752-1688.2011.00541.x.

846 Vogt, J., Soille, P., De Jager, A., Rimaviciute, E., Mehl, W., Foisneau, S., Bodis, K., Dusart, J.,
847 Paracchini, M.L., Haastrup, P., Bamps, C., 2007. A pan-European River and Catchment
848 Database. *OPOCE*. doi:10.2788/35907.

849 Von Storch, H., 1999. Misures of Statistical Analysis in Climate Research. Analysis of Climate
850 Variability: *Applications of Statistical Techniques Proceedings of an Autumn School Organized*

851 *by the Commission of the European Community on Elba from October 30 to November 6, 1993,*
852 11–26. doi:10.1007/978-3-662-03744-7_2.

853 Vormoor, K., Lawrence, D., Schlichting, L., Wilson, D., Wong, W.K., 2016. Evidence for
854 changes in the magnitude and frequency of observed rainfall vs. snowmelt driven floods in
855 Norway. *Journal of Hydrology* **538**, 33–48. doi:10.1016/j.jhydrol.2016.03.066.

856 WMO, 2009. Extreme value analysis, in: WMO Commission for Hydrology (Ed.), Management
857 of Water Resources and Application of Hydrological Practices, 1–59.

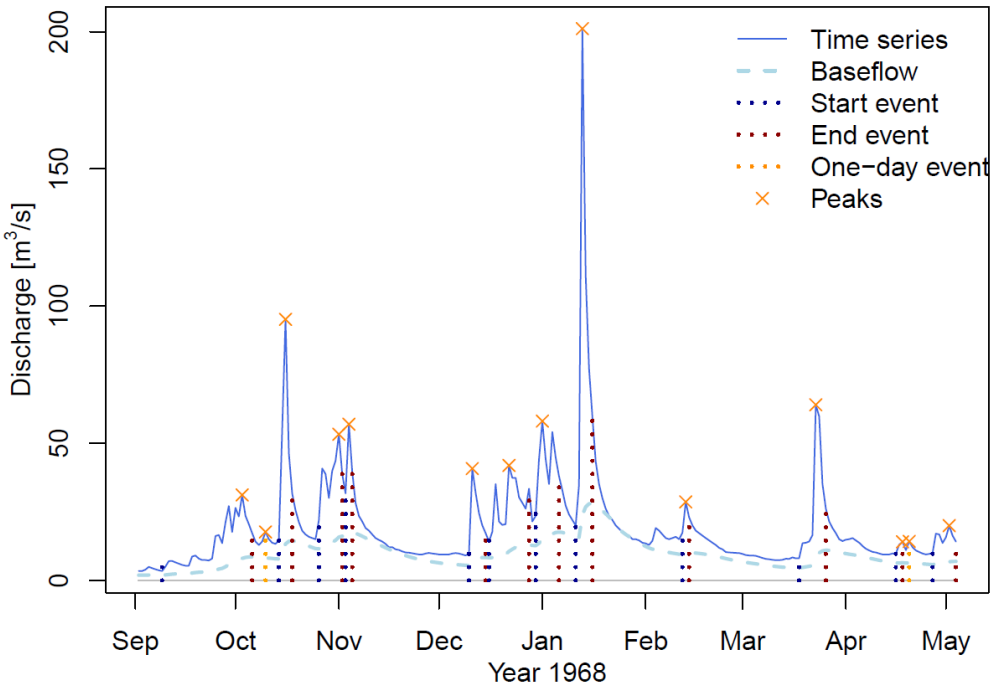

858

859 Figure 1. Example of discharge events and peak flows (crosses) for river Teme,
860 at Tenbury station (UK). A discharge event starts (vertical dashed dark blue line) when
861 the direct runoff is larger than the baseflow (light blue dashed line), and ends (vertical
862 dashed red line) when it is lower. One-day long events are shown with vertical dashed
863 orange lines, independent peak discharges as orange crosses.

864

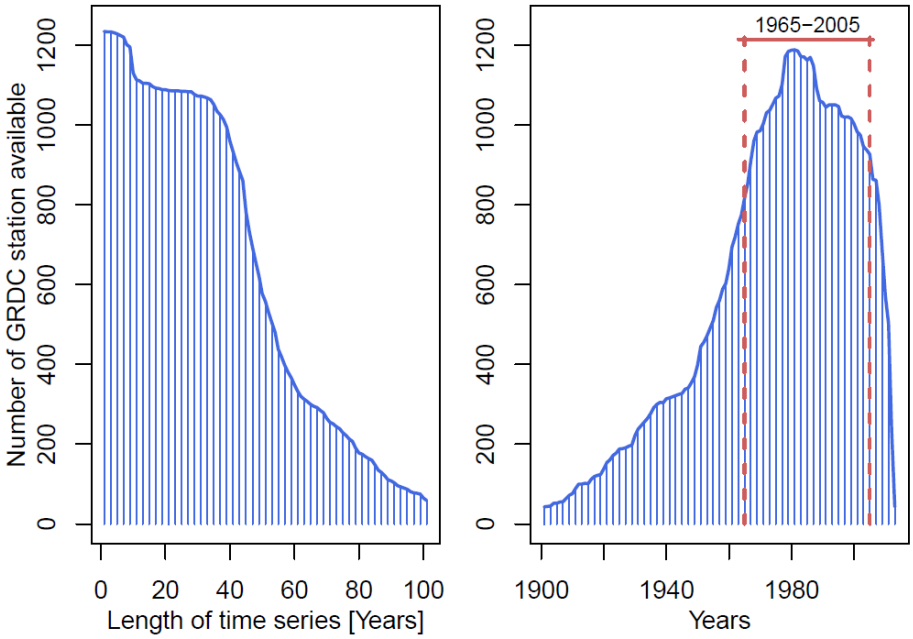

Figure 2. Length and time periods of daily discharge time series contained in the European Global Runoff Data Centre (GRDC) subset. Left panel shows the time series length. Right panel shows the number of stations, which have data available in that year for the period 1900-2010. Red lines indicate the time window 1965-2005 selected for the trend analysis.

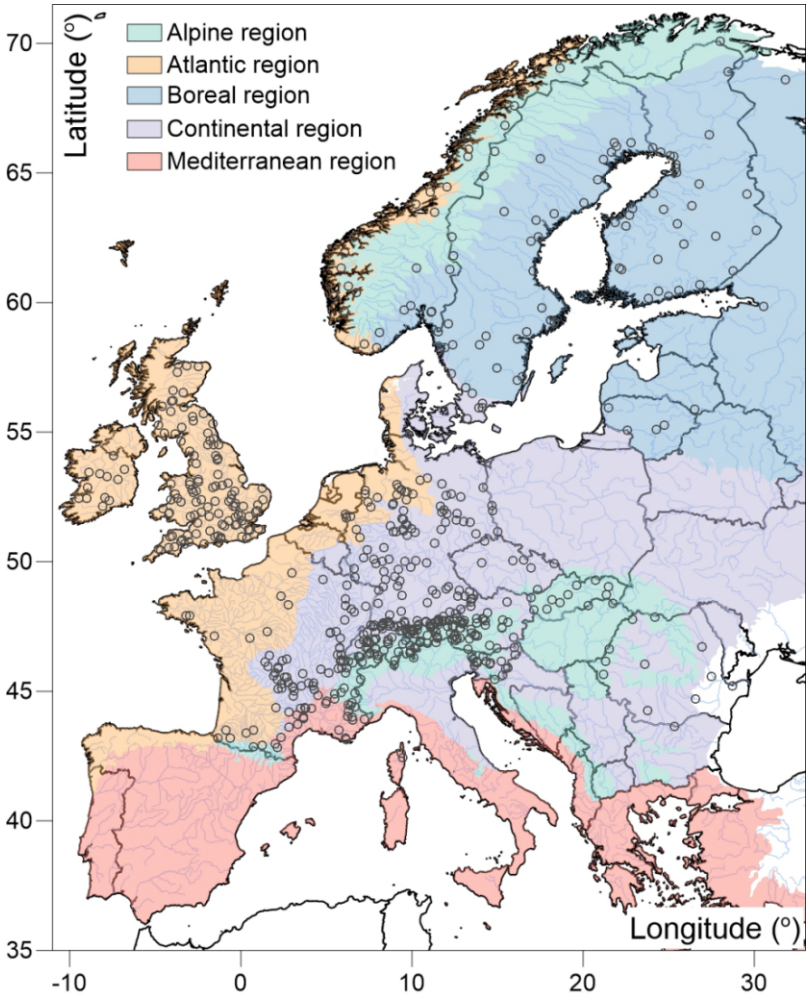

872

873 Figure 3: Five hydro-climatic regions in Europe based on a bio-geographical

874 classification provided by the EEA. Points indicate the location of the 629 gauging

875 stations.

876

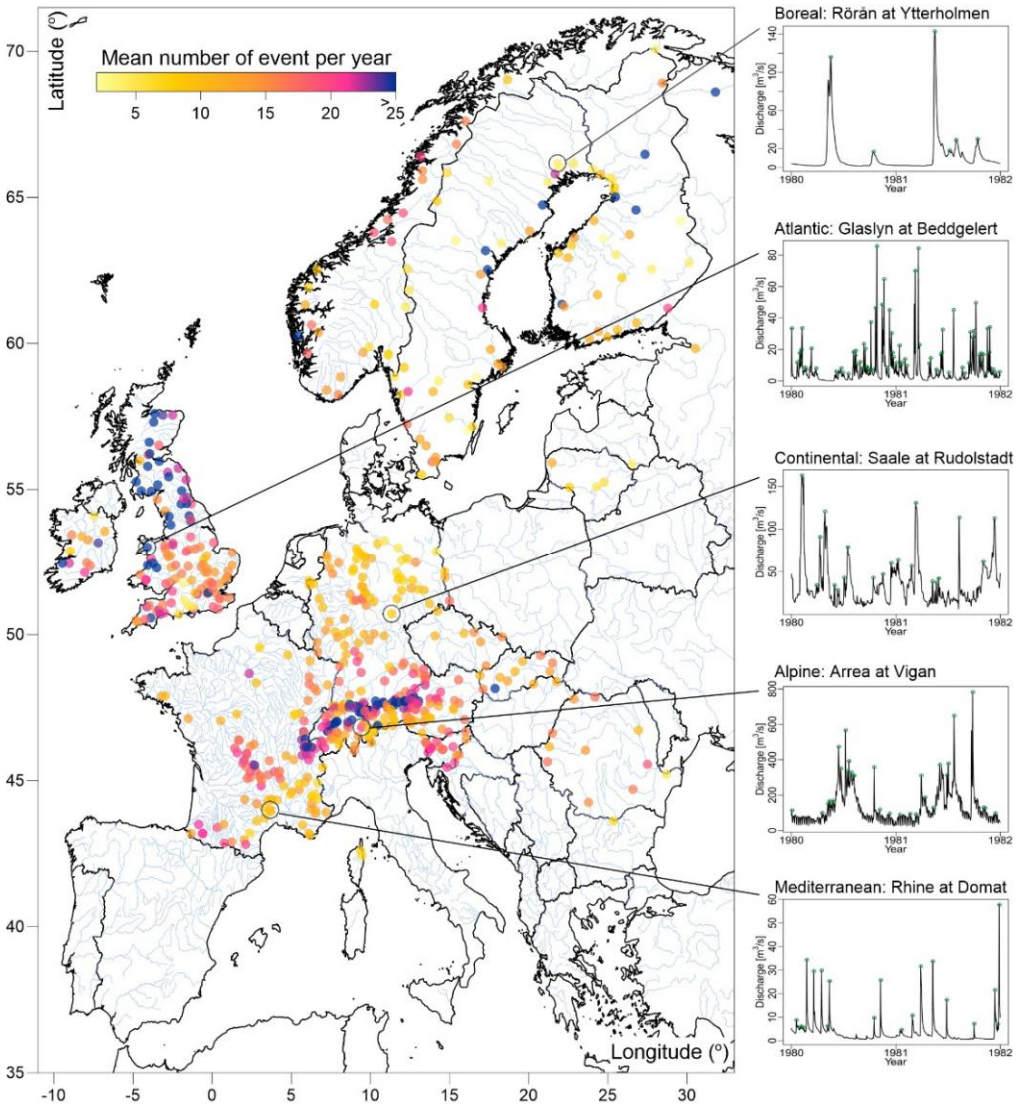

877

878 Figure 4. Mean number of independent discharge peaks per year at the selected

879 629 GRDC gauging stations. Panels on the right show examples of runoff hydrographs

880 and discharge peaks for five sample gauging stations in the five hydro-climatic regions.

881

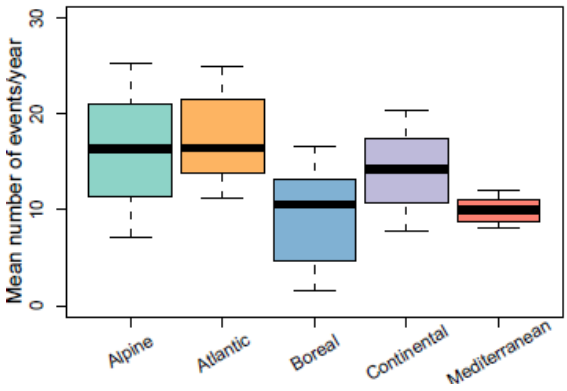

Figure 5. Mean number of independent discharge peaks per year identified by the baseflow-based algorithm, for each of the five hydro-climatic region. Bold line represents the 50% percentile, while boxes and whiskers show the 25%-, 75%-percentile, and the 10%-, 90%- percentiles, respectively.

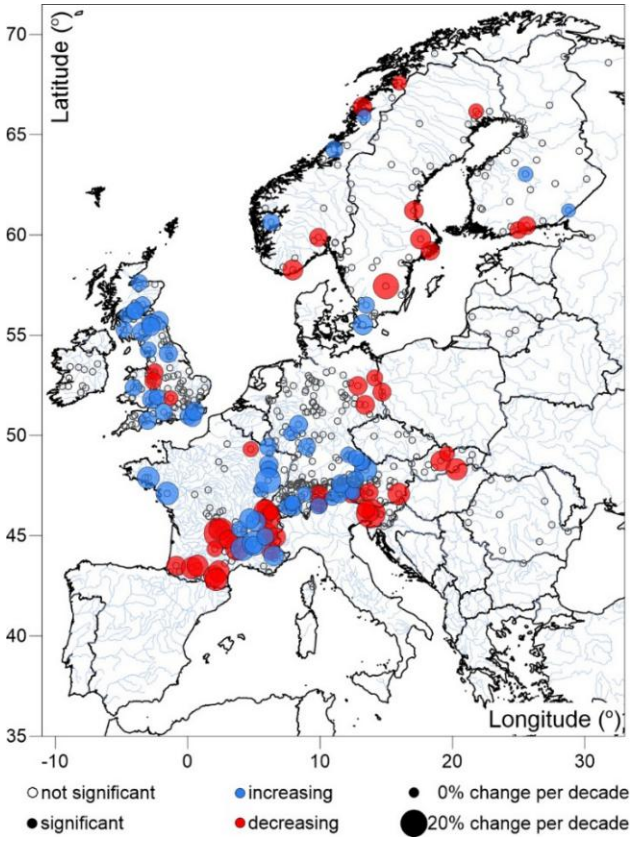

890

891 Figure 6. Trends in Annual Maximum Flood series (AMF) for the period 1965-
892 2005. Filled symbols indicate statistical significant positive (blue) and negative (red)
893 trends at 10% level of significance. Symbol size indicates the magnitude of change in
894 the mean flood magnitude (% per decade).

895

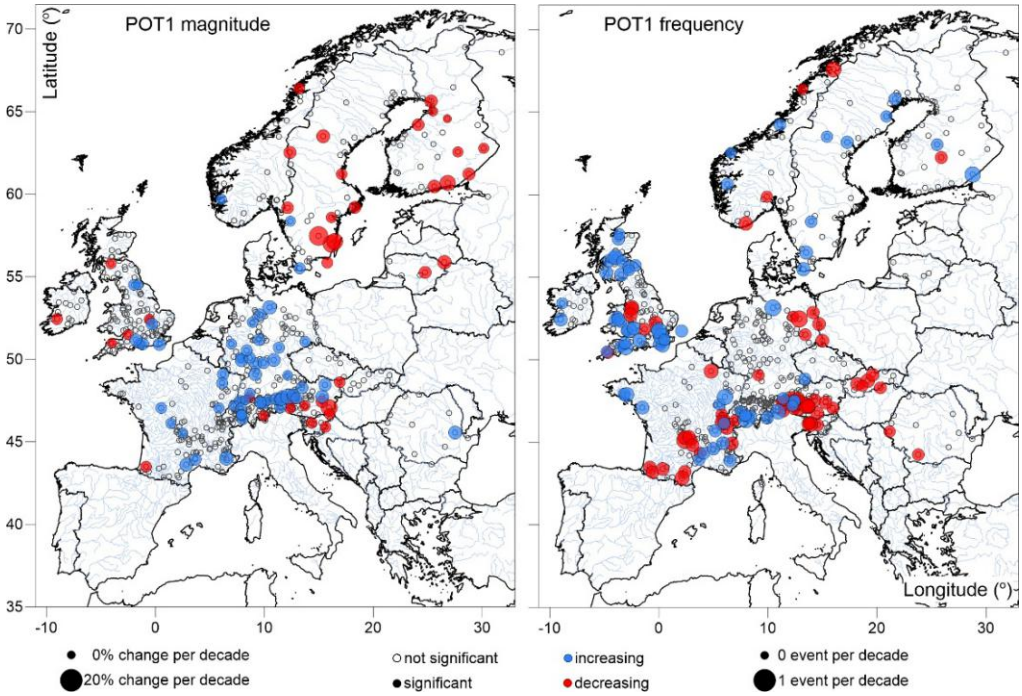

Figure 7. Trends in POT1 series. Left/right panel shows trends in flood magnitude/frequency. Filled symbols indicate statistical significant positive (blue) and negative (red) trends at 10% level of significance. Symbol size indicates the change in the mean flood magnitude (left), mean number of floods (right) exceeding the threshold in % per decade and in events per decade respectively.

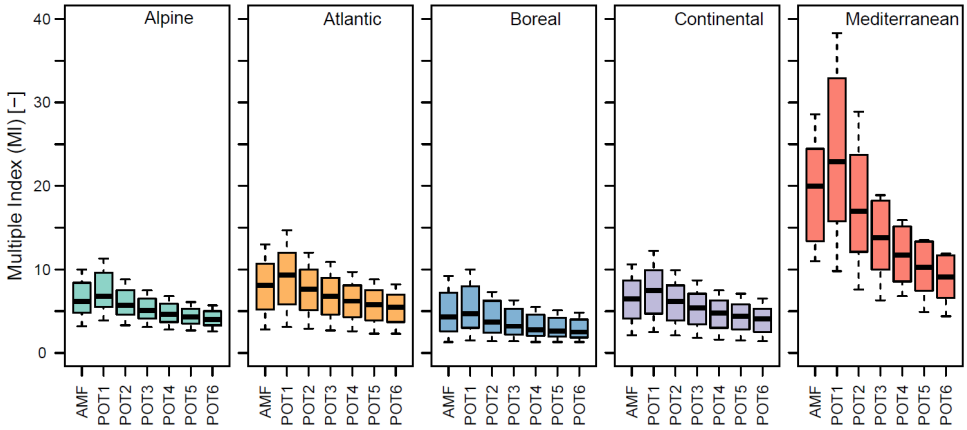

906

907 Figure 8. Multiple Index (MI) of the Annual Maximum Flood (AMF) and the

908 different Peak Over Threshold (POT) flood series. For the latter thresholds of λ (mean

909 number of peaks per year) are ranging from 1 (POT1) to 6 (POT6).

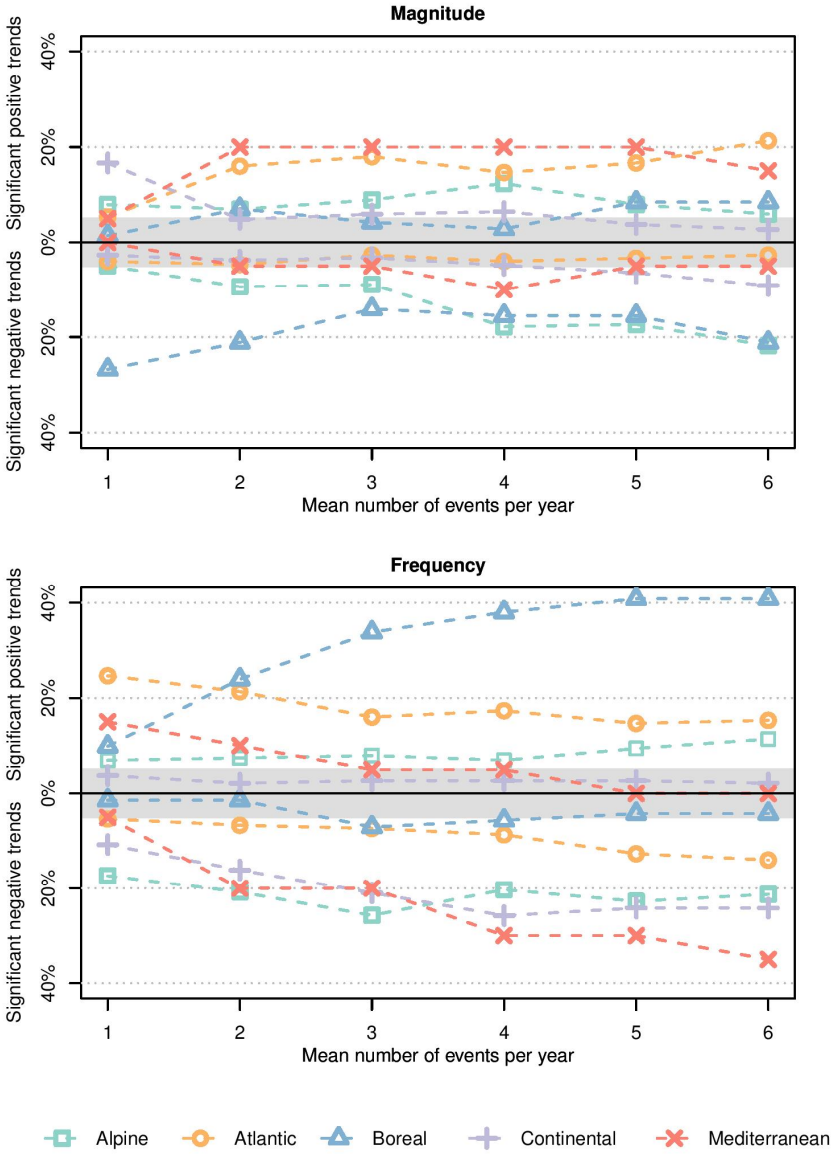

910

911 Figure 9. Percentage of stations exhibiting significant trends in magnitude and
912 frequency at 10% level, with a threshold λ ranging from a mean of one to six
913 events/year. Top and bottom panel show the sensitivity analysis in flood magnitude and
914 frequency, respectively. Different colours and symbols indicate the 5 hydro-climatic
915 regions. The grey band represents the percentage of station (5% in the positive semiaxis
916 and 5% negative semiaxis) exhibiting trend that is expected to be detected by chance,
917 given the significance level of the test.

918

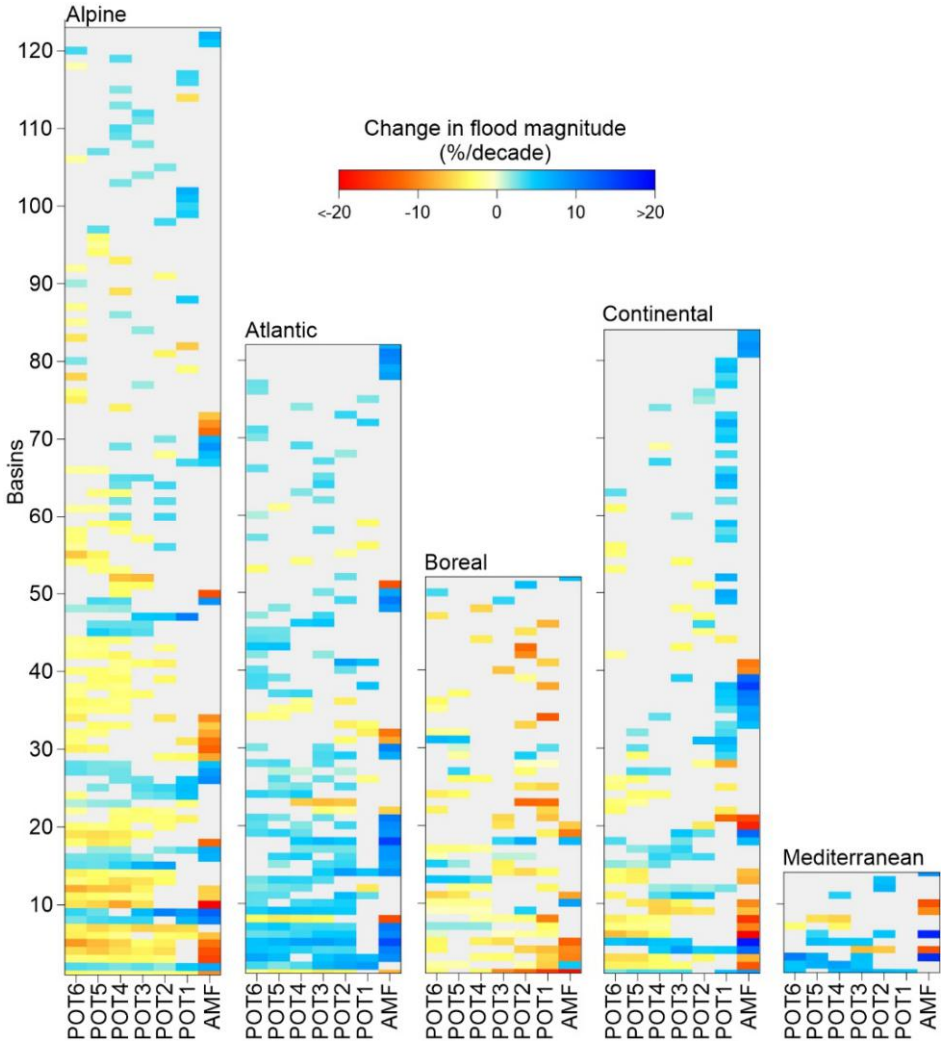

Figure 10. Summary of the significant trends detected at 10% level in the AMF and the POT-M series. POT-M series are compiled for a mean number of exceedances λ ranging from 1 to 6. The colour scale indicates the intensity of the decadal change detected for significant trends, in % per decade, while grey colour is used when no significant trends are detected. Catchments are grouped into the five hydro-climatic regions of Europe and are sorted in a decreasing order (from the bottom) by the cumulative number significant trends detected in individual catchments over the different flood series.

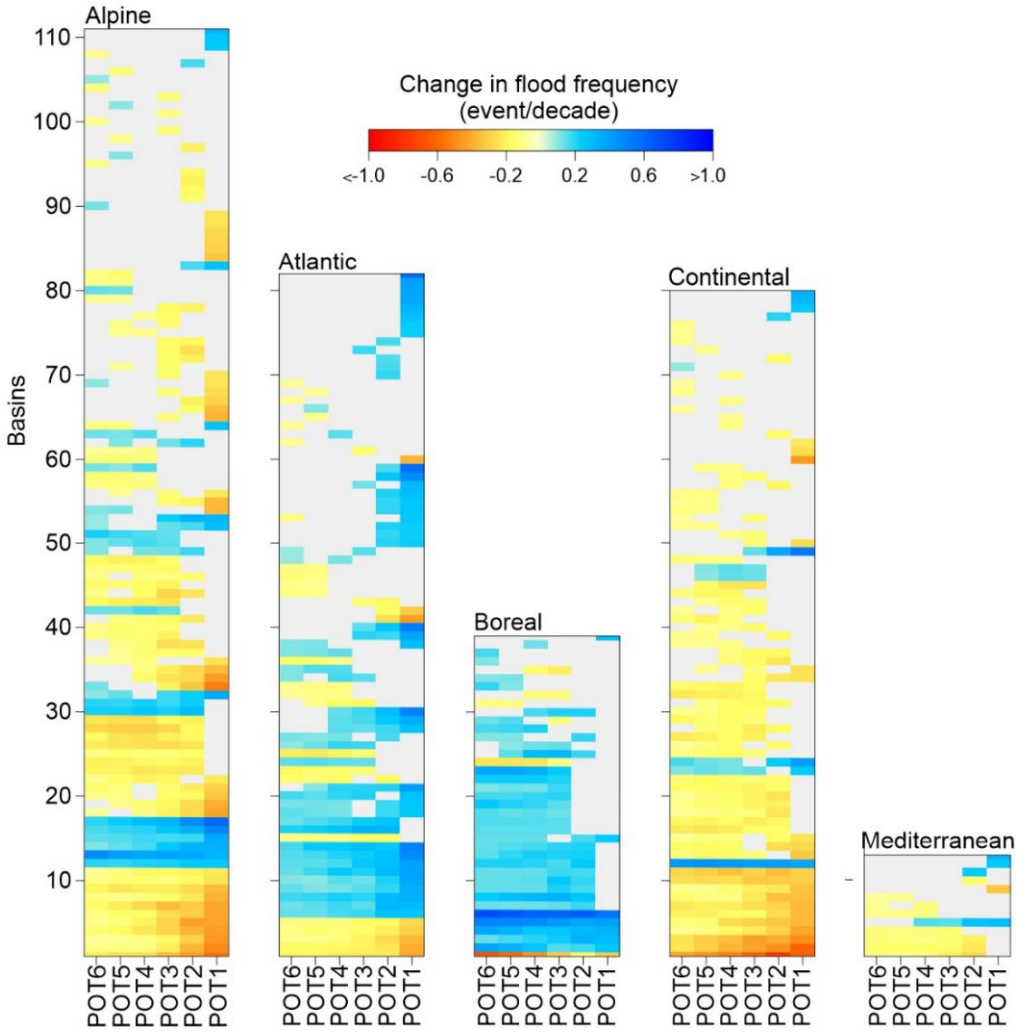

930

931 Figure 11. Summary of the significant trends detected at 10% level in the POT-F
932 series. POT-F series are compiled for a mean number of exceedances λ ranging from 1
933 to 6. The colour scale indicates the intensity of the decadal change detected for
934 significant trends, in % per decade, while grey colour is used when no significant trends
935 are detected. Catchments are grouped into the five hydro-climatic regions of Europe and
936 are sorted in a decreasing order (from the bottom) by the cumulative number significant
937 trends detected in individual catchments over the different flood series.

938

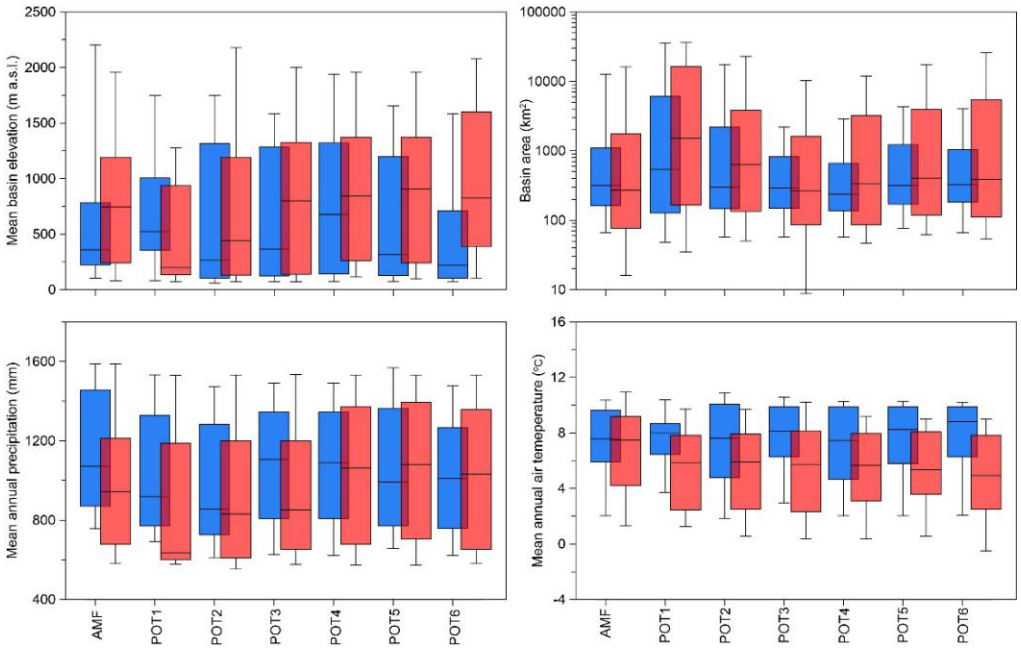

939

940 Figure 12. Distribution of selected physiographic characteristics of the

941 catchments exhibiting significant trends in flood magnitude at 10% level. Increasing or

942 decreasing trends in flood magnitude are presented in blue or red colour, respectively.

943 Bold lines represent the 50%- percentile, while boxes and whiskers indicate the 10%-,

944 25%-, 75%- and 90%- percentiles.

945

946

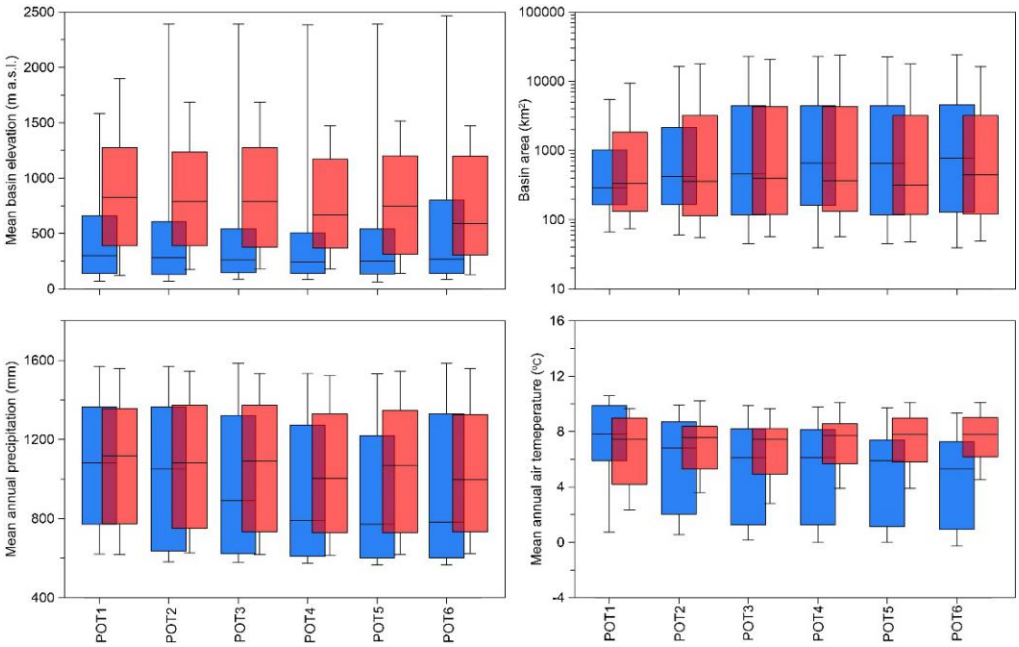

947

948 Figure 13. Distribution of selected physiographic characteristics of the

949 catchments exhibiting significant trends in flood frequency at 10% level. Increasing or

950 decreasing trends in flood magnitude are presented in blue or red colour, respectively.

951 Bold lines represent the 50%- percentile, while boxes and whiskers indicate the 10%-,

952 25%-, 75%- and 90%- percentiles.

953

954

955

956

957

958

959

960

961 Table 1: Description of the five hydro-climatic regions (see also Fig. 3). The table
962 contains the name of the regions, the main geographical position, number of stations
963 located within, the CCM2 windows that cover the region and the predominant Köppen-
964 Geiger climate classification.

Region	Geographical position	Number of stations	CCM2 windows	Predominant Köppen climate
Alpine	Central range systems	202	2000, 2002, 2003, 2005, 2007, 2008	Snow and polar
Atlantic	Northern islands/coasts	150	2000, 2001, 2003, 2008	Warm temperate - fully humid
Boreal	Northern Europe	71	2000, 2007, 2008, 2013	Snow - fully humid
Continental	Central Europe	186	2000, 2003, 2005, 2013	Warm temperate and snow - fully humid
Mediterranean	Southern Europe	20	2002, 2003	Warm temperate - summer dry

965
966
967
968
969
970
971
972
973
974

975 Table 2. Absolute number of stations exhibiting significant positive/negative
976 trends at 10% level in flood magnitude detected in the POT-M series with a thresholds
977 λ (a mean number of events per year) ranging from 1 (POT1-M) to 6 (POT6-M). The
978 stations are grouped into the different hydro-climatic regions.

	Alpine	Atlantic	Boreal	Continental	Mediterranean
Number of stations	202	150	71	186	20
POT1-M	16/10	8/6	1/19	31/5	1/0
POT2-M	14/19	24/7	5/15	9/7	4/1
POT3-M	18/18	27/4	3/10	11/6	4/1
POT4-M	25/36	22/6	2/11	12/9	4/2
POT5-M	16/35	25/5	6/11	7/12	4/2
POT6-M	12/44	32/4	6/15	5/17	3/1

979
980
981 Table 3. Absolute number of stations exhibiting significant positive/negative
982 trends at 10% level in flood frequency detected in the POT-F series with a thresholds λ
983 (a mean number of events per year) ranging from 1 (POT1-F) to 6 (POT6-F). The
984 stations are grouped into the different hydro-climatic regions.

	Alpine	Atlantic	Boreal	Continental	Mediterranean
Number of stations	202	150	71	186	20
POT1-F	14/35	37/8	7/1	7/20	3/1
POT2-F	15/42	32/10	17/1	4/30	2/4
POT3-F	16/52	24/11	24/5	5/39	1/4
POT4-F	14/41	26/13	27/4	5/48	1/6
POT5-F	19/46	22/19	29/3	5/45	0/6
POT6-F	23/43	23/21	29/3	4/45	0/7

985